



Pergamon

SCIENCE @ DIRECT®

Tetrahedron: *Asymmetry* 14 (2003) 1141–1152TETRAHEDRON:
ASYMMETRY

Efficient enantiodiscrimination of chiral monophosphine oxides and boranes by phosphorus coupled ^{13}C NMR spectroscopy in the presence of chiral ordering agents

Michaël Rivard,^a Frédéric Guillen,^a Jean-Claude Fiaud,^{a,*} Christie Aroulanda^b and Philippe Lesot^{b,*}^aLaboratoire de Catalyse Moléculaire, CNRS UMR 8075, ICMMO, Bât. 420, Université de Paris-Sud, 91405 Orsay, France^bLaboratoire de Chimie Structurale Organique, CNRS UMR 8074, ICMMO, Bât. 410, Université de Paris-Sud, 91405 Orsay, France

Received 18 December 2002; accepted 24 February 2003

Abstract—The synthesis of new chiral phospholanes via the corresponding oxides or boranes is reported and the analytical potential of ^{13}C - $\{^1\text{H}\}$ NMR spectroscopy in weakly ordering polypeptide liquid crystalline phases in view to differentiate between enantiomers of these chiral phosphines precursors is explored. In particular results involving organic solutions of poly- γ -benzyl-L-glutamate (PBLG) and poly- ϵ -carbobenzyloxy-L-lysine (PCBLL) are described. This NMR approach allows determination of the enantiomeric composition, and provides therefore a new efficient alternative to classical methods usually used to analyze this class of compounds. A description of various spectral enantiodifferentiation patterns expected to be observed using ^{13}C - $\{^1\text{H}\}$ NMR of enantiomers having a spin-1/2 heteroatomic nucleus, embedded in a chiral liquid crystal is presented. © 2003 Elsevier Science Ltd. All rights reserved.

1. Introduction

Biphosphine ligands have proved to be among the most successful ligands for enantioselective transition-metal catalysis. However, the interest of monophosphines in asymmetric catalysis has seen a resurgence of interest.¹ Indeed some transition-metal catalyzed reactions have been reported for which monophosphines ligands were more active and enantioselective than numerous diphosphines.² On the other hand, chiral, basic monophosphines have been described as being useful nucleophilic catalysts³ for kinetic resolutions of racemic secondary alcohols through acylation,⁴ in cycloadditions of dienones with electron-deficient olefins⁵ and imines,⁶ and in γ -addition reactions to acetylenic esters.⁷

We recently described the synthesis of 1,2-*c*,5-*t*-triphenylphospholane **4a** via the corresponding oxide **3a** and reported preliminary results on the use of this monophosphine as a chiral ligand in rhodium-catalyzed

enantioselective hydrogenation of olefinic compounds.⁸ The preparation of the oxide (*S,S*)- or (*R,R*)-**3a** is possible from the (*S,S*)- or (*R,R*)-phosphinic acid **1**, respectively as shown in the general synthetic Scheme 1 (only compounds with 2*S*,5*S* configuration are depicted). Following the same or a modified procedure (using phosphine borane such as **6** instead of phosphine oxide **3**), our aim was then to enlarge the range of monophosphines accessible from **1**, such as nucleophilic phospholanes **4b**⁸ or **4c**.

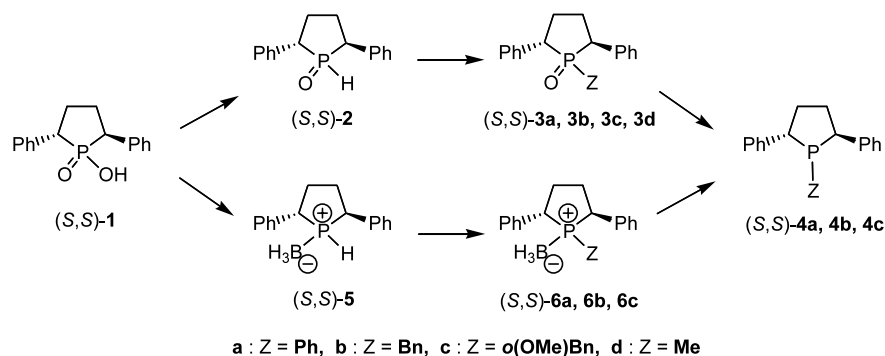
In the course of our studies an important point concerned the measurement of the enantiomeric purity of our compounds. Considering the synthetic route described in Scheme 1, the preparation of either **3** or **6** was critical. Indeed the use of *n*-butyllithium or hydride as base to create a nucleophilic phosphorus species could induce the total or partial loss of chirality (due to the acidic positions 2 and 5 in the heterocyclic ring⁹). To ascertain the configurational integrity of the phospholane frame, numerous analytical methods to measure the e.e. of compounds **3** or **6** can be explored.¹⁰ Nevertheless, previous work showed that analysis by HPLC of scalemic mixtures of **3a** was delicate to perform and,¹¹ in our hands, no satisfactory results were

* Corresponding authors. (Jean-Claude Fiaud for the chemistry; Philippe Lesot for the NMR in oriented solvents); e-mail: fiaud@icmo.u-psud.fr; philesot@icmo.u-psud.fr

obtained using conventional HPLC. Furthermore, no spectroscopic methods¹² (using chiral shift reagent (CLSR) or chiral solvating agents (CSAs)) were suitable, to our knowledge, to spectroscopically resolve both chiral phosphine oxides and phosphine boranes. In this context, we turned our attention to NMR spectroscopy in the presence of chiral ordering agents (COA) provided by weakly ordering polypeptidic chiral liquid crystals (CLC's).^{13,14}

The first advantage of the COAs method compared with the previous analytical approaches is that no specific chemical functionalities or molecular topologies¹⁵ in the compounds under investigation are required. Indeed only the selective orientational ordering of two enantiomers inside the chiral oriented phase induces the enantiomeric discrimination.¹⁶ The second advantage is that NMR spectroscopy provides basically numerous efficient tools to differentiate between the signals of enantiomers. Indeed any magnetically active nuclei present in the molecule under study is a potential NMR probe for our purpose.¹³ In this work we have exploited the potential of proton decoupled ¹³C NMR (¹³C-¹H} NMR)^{17,18} using organic solutions of poly- γ -benzyl-L-glutamate (PBLG) and poly- ϵ -carbobenzyl-oxy-L-lysine (PCBL)¹⁴ to enantiodiscriminate the signal of chiral monophosphine derivatives.

This paper describes new chemical syntheses of monophosphine derivatives and spectroscopic analyses of this class of chiral compounds using NMR in CLC's. It will be presented as following. In the first part, we propose an extended description of ¹³C-¹H} NMR spectroscopy of enantiomers having a full abundant spin-1/2 heteroatomic nucleus, such as a phosphorus atom, embedded in a polypeptide CLC. In particular we analyze the various possible spectral enantiodifferentiation patterns expected to be observed for any carbon nucleus. Next, we describe the synthesis of new chiral phospholanes via the corresponding chiral monophosphine boranes as well as the corresponding chiral monophosphine oxides. Finally we report and discuss the enantiomeric discrimination observed for **3b**, **3c**, **3d** and **6b** in racemic and optically active series.



Scheme 1.

2. Results and discussion

2.1. Theoretical description of ¹³C-¹H} NMR spectroscopy of enantiomers having a spin-1/2 heteroatomic nucleus in weakly ordered CLC's

In a chiral anisotropic phase, the NMR resonance frequency, $\nu_{^{13}\text{C}}$, of a non coupled ¹³C nucleus contains both an isotropic, $\sigma_{^{13}\text{C}}^{\text{iso}}$, and an anisotropic contribution, $\Delta\sigma_{^{13}\text{C}}$, to the electronic shielding and may be expressed for two enantiomers such as:^{13,19}

$$\nu_{^{13}\text{C}}^{S \text{ or } R} = \frac{\gamma_{^{13}\text{C}}}{2\pi} [1 - \sigma_{^{13}\text{C}}^{\text{iso}} - \Delta\sigma_{^{13}\text{C}}^{S \text{ or } R}] B_0 \quad (1)$$

where $\gamma_{^{13}\text{C}}$ is the magnetogyric ratio of ¹³C nucleus. Expressed in a molecular frame (a,b,c), the terms $\sigma_{^{13}\text{C}}^{\text{iso}}$ and $\Delta\sigma_{^{13}\text{C}}^{S \text{ or } R}$ are defined as:

$$\sigma_{^{13}\text{C}}^{\text{iso}} = \frac{1}{3}(\sigma_{\text{aa}} + \sigma_{\text{bb}} + \sigma_{\text{cc}}) \text{ and} \quad \Delta\sigma_{^{13}\text{C}}^{S \text{ or } R} = \frac{2}{3} \sum_{\alpha, \beta = \text{a, b, c}} \sigma_{\alpha\beta} S_{\alpha\beta}^{S \text{ or } R} \quad (2)$$

where $S_{\alpha\beta}^{S \text{ or } R}$ is the Saupe's matrix that describes the molecular orientational order of *S* and *R* isomers.

Eq. (1) indicates that enantiomeric discrimination of such a nucleus can be detected if $\nu_{^{13}\text{C}}^S - \nu_{^{13}\text{C}}^R \neq 0$. In practice when the term $\Delta\sigma_{^{13}\text{C}}^S$ significantly differs from $\Delta\sigma_{^{13}\text{C}}^R$, two resolved NMR resonances instead of a single one are observed in chiral oriented solvents. The term $\Delta\sigma_{^{13}\text{C}}^{S \text{ or } R}$ depends both upon the difference in order parameters between enantiomers and the electronic shielding anisotropy of a ¹³C nucleus.¹³ Generally the magnitude of the electronic shielding anisotropy is rather small, but nuclei having largest chemical shift anisotropies such as *sp* or *sp*² carbon atoms^{13,18} may provide an efficient probe allowing enantiomers to be discriminated on the basis of a chemical shift anisotropy difference in ¹³C-¹H} NMR spectroscopy in a CLC.

The presence in a chiral molecule of a spin-1/2 heteroatomic nucleus X (and 100% abundant), such as ³¹P

or ^{19}F atom, in the compounds may significantly complicate the analysis of ^{13}C - $\{^1\text{H}\}$ NMR spectra by the presence of short and long-range ^{13}C -X dipolar couplings (noted $D_{^{13}\text{C}-\text{X}}$). The most straightforward solution to simplify such analysis consists of simultaneously decoupling both the signals of the protons and the X-nucleus. This type of NMR experiments will be denoted hereafter ^{13}C - $\{^1\text{H}, \text{X}\}$ where X is the second heteroatom decoupled. This experimental procedure is, however, only possible when two X-channels are set in the NMR spectrometer hardware and obviously requires an adequate triple resonance NMR probe (e.g. ^1H , ^{13}C , X). In this case the first X-channel allows observation of the carbon nuclei, the second one is then dedicated to the decoupling of the X-nuclei. Unfortunately, the majority of routine spectrometers used to date in organic chemistry laboratories do not possess such capabilities, and hence the simultaneous decoupling of protons and other active heteroatomic nuclei is often precluded. On the other hand, disregarding the complexity of the proton decoupled, X-coupled ^{13}C spectra, the presence of a further spin-1/2 heteronucleus X in molecules implies the existence of dipolar couplings ^{13}C -X which can be very useful for differentiating the NMR signals of two enantiomers, in particular when $\nu_{^{13}\text{C}}^{\text{S}} - \nu_{^{13}\text{C}}^{\text{R}} \approx 0$.

In the phosphorus coupled, proton decoupled ^{13}C spectra of enantiomers dissolved in a CLC, dipolar interactions between ^{13}C and ^{31}P atoms are not averaged to zero. In this case each pair of interacting ^{13}C and ^{31}P nuclei for both isomers may produce a direct dipolar coupling, $D_{^{13}\text{C}-^{31}\text{P}}$, defined in Hz unit as:¹³

$$D_{^{13}\text{C}-^{31}\text{P}}^{\text{S or R}} = -k_{^{13}\text{C}-^{31}\text{P}} \left\langle \frac{S_{^{13}\text{C}-^{31}\text{P}}^{\text{S or R}}}{r_{^{13}\text{C}-^{31}\text{P}}^3} \right\rangle \text{ with } k_{^{13}\text{C}-^{31}\text{P}} = \frac{h\gamma_{^{13}\text{C}}\gamma_{^{31}\text{P}}}{4\pi^2} \quad (3)$$

In this equation, h is the Planck's constant, $\gamma_{^{31}\text{P}}$ is the magnetogyric ratio of ^{31}P nucleus, the angular brackets denote an (ensemble or time) average over molecular tumbling and internal motions (vibrational motions, conformational changes...), $r_{^{13}\text{C}-^{31}\text{P}}$ is the internuclear distance and $S_{^{13}\text{C}-^{31}\text{P}}^{\text{S or R}}$ is the orientational order parameter of the internuclear direction ^{13}C - ^{31}P . Disregarding any discrepancies in the molecular geometry between the enantiomers, Eq. (3) shows that the spectroscopic enantiodiscrimination on the basis of ^{13}C - ^{31}P dipolar couplings, occurs when the $S_{^{13}\text{C}-^{31}\text{P}}$ parameter is different for the S and R isomers. In practice, the spectroscopic separations using dipolar couplings are visible in the spectra through the doubling of coupling structures, one for each enantiomer.

From a spectroscopic point of view, the interpretation of proton decoupled, phosphorus coupled ^{13}C spectra in oriented phase is very similar to the analysis which can be made in isotropic solvents. The main difference is that the splittings between resonances in first order coupling structures, are now equal to:^{13,17}

$$T_{^{13}\text{C}-^{31}\text{P}} = J_{^{13}\text{C}-^{31}\text{P}} + 2D_{^{13}\text{C}-^{31}\text{P}} \quad (4)$$

where $J_{^{13}\text{C}-^{31}\text{P}}$ is the isotropic part of the scalar coupling (its anisotropic part is neglected) and $D_{^{13}\text{C}-^{31}\text{P}}$ is the dipole-dipole contribution. $T_{^{13}\text{C}-^{31}\text{P}}$ is referred to as the total spin-spin coupling between a phosphorus and ^{13}C atom. As the sign of $D_{^{13}\text{C}-^{31}\text{P}}$ can be negative or positive, the first order splitting for a pair of interacting ^{13}C and ^{31}P nuclei may be zero when $J_{^{13}\text{C}-^{31}\text{P}} = -2D_{^{13}\text{C}-^{31}\text{P}}$, thus producing a fortuitous decoupling. This situation is often encountered for weakly ordering liquid crystals such as organic solutions of PBLG or PCBL because in this case, dipolar and scalar couplings can be of the same order of magnitude. Finally it can be noted from Eq. (3) that the ^{13}C - ^{31}P dipolar couplings are dependent on the internuclear distance between the ^{13}C and ^{31}P nuclei. They can be observed between two directly bonded nuclei or between nuclei relatively far from each other in the structure.

The spectroscopic features of proton decoupled, ^{31}P coupled ^{13}C NMR signals are governed both by the magnitude of ^{13}C - ^{31}P total spin-spin couplings for each isomer as well as the difference of ^{13}C chemical shift anisotropy associated with a given carbon atom. Actually the magnitude of chemical shift anisotropy difference for a carbon atom can be larger, equal or smaller than its ^{13}C - ^{31}P total spin-spin couplings. As a consequence, various spectral enantiodifferentiation patterns depending on the relative magnitude of anisotropic interactions exist for a pair of interacting ^{13}C - ^{31}P nuclei. To illustrate our purpose, Figures 1 and 2 schematically depict the different possible spectral patterns encountered on the ^{13}C - $\{^1\text{H}\}$ and ^{13}C - $\{^1\text{H}, ^{31}\text{P}\}$ NMR spectra of a racemic mixture of enantiomers having a single phosphorus nucleus. Obviously these ^{13}C spectral situations can be detected with any other spin $I=1/2$ heteroatomic nucleus X (100% abundant) contained in the chiral molecule.

For the sake of clarity, the various spectral enantiodifferentiation patterns depicted have been categorized in two classes, corresponding to the cases where the difference of chemical shift anisotropy ($\Delta\Delta\sigma$) is null (series a) and the cases where $\Delta\Delta\sigma \neq 0$ (series b, c, d and e). For the latter cases, various sub-categories can arise depending on the relative magnitude of the total coupling $T_{^{13}\text{C}-^{31}\text{P}}$ for the enantiomer R (T^{R}), and for the enantiomer S (T^{S}) compared with $\Delta\Delta\sigma$. Thus, the series b shows the spectral diagrams in which T^{R} is equal to zero. The series c presents the spectral diagrams expected to be observed when T^{R} and T^{S} are both larger than $\Delta\Delta\sigma$. The series d groups the spectral diagrams expected to be observed when T^{R} and T^{S} are smaller than or equal to the difference of chemical shift anisotropy. Finally in the last series e we describe the cases for which T^{R} is smaller than $\Delta\Delta\sigma$, while T^{S} is larger than $\Delta\Delta\sigma$. Note that for all series, we have arbitrarily assumed that the ^{13}C signal of the S enantiomer was deshielded in regards to the R enantiomer. Experimentally the opposite situation exists (as we will see experimentally below), but unfortunately it is not predictable. This is because, to date, there is no simple correlation between the R/S (or \pm) descriptors, the chemical class of enantiomers studied and the magni-

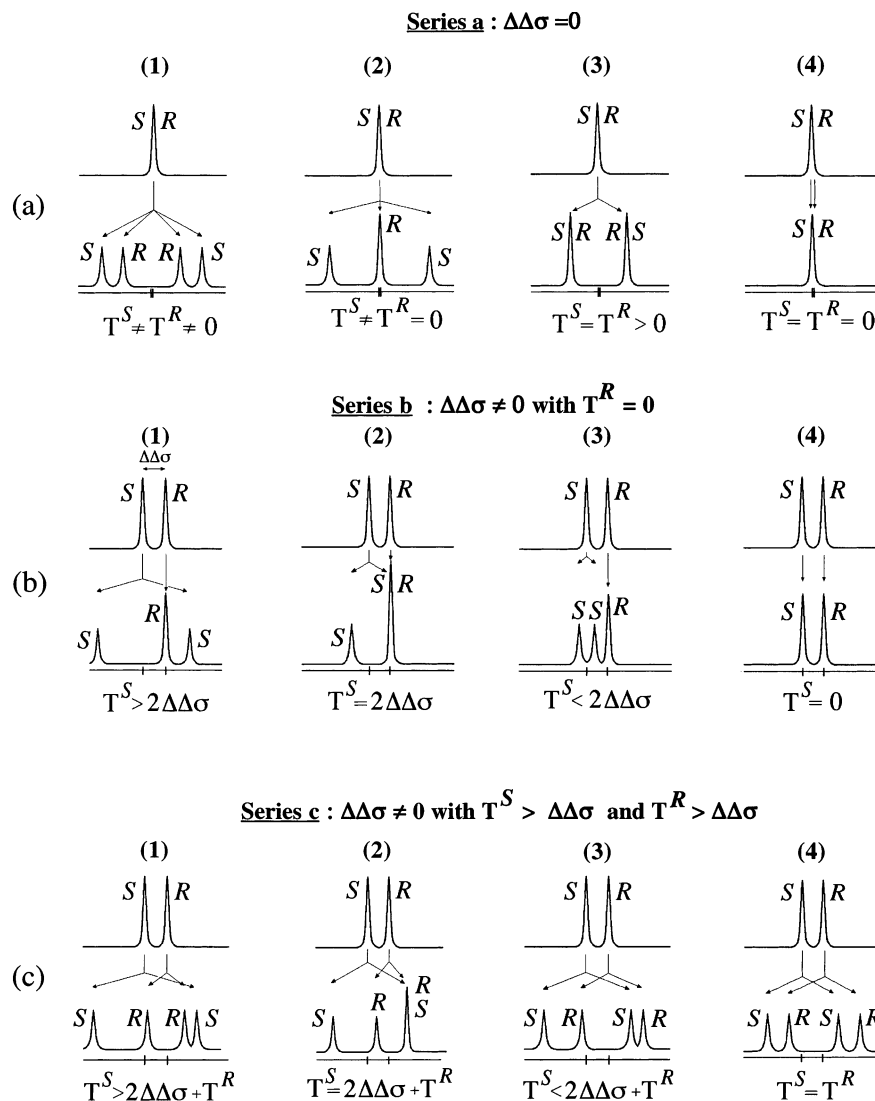


Figure 1. Schematic representation (series a, b and c) of possible enantiodifferentiation spectral patterns expected to be observed on the $^{13}\text{C}\text{-}\{^1\text{H}, \text{X}\}$ NMR spectra (top row) and $^{13}\text{C}\text{-}\{^1\text{H}\}$ NMR spectra (bottom row) of enantiomers (racemic mixture) having a single spin-1/2 heteroatomic nucleus (noted X) with spin $I=1/2$, and embedded in a chiral liquid crystal. When existing, the chiral differentiation is based on a difference of the chemical shift anisotropies, $\Delta\Delta\sigma = |\Delta\sigma_{^{13}\text{C}}^{\text{S}} - \Delta\sigma_{^{13}\text{C}}^{\text{R}}|$, and/or the $^{13}\text{C}\text{-X}$ total couplings, T^{S} or T^{R} .

tude of chemical shift anisotropy for a given carbon atom. For each series, we present different spectral patterns corresponding to the various possible situations depending now on the relative magnitudes of T^{S} and T^{R} . For simplicity, these different cases will be numbered from a to e and, for each series, from 1 to 3, 4 or 5.

Several comments can be drawn from the examination of all the various spectral patterns given in Figures 1 and 2. First of all, we can see the diversity of ^{13}C spectral patterns. Thus, the patterns a-1 and a-2 illustrate the possibility to differentiate between the signal of two enantiomers on the exclusive basis of $^{13}\text{C}\text{-X}$ dipolar couplings ($\Delta\Delta\sigma = 0$). In contrast the pattern b-4 shows the possibility to discriminate the two enantiomers on the exclusive basis of the ^{13}C chemical shift anisotropy ($T = 0$). This situation perfectly reflects the versatility of chiral discrimination in CLC's when two anisotropic

observables govern the spectral features. It also proves the undeniable advantage of the NMR in oriented solvents that is susceptible to combine different anisotropic observables useful in the field of the enantiomeric analysis. The second remark concerns the probability to observe experimentally one of these patterns. Although no situations can be a priori excluded, some of them should be rarely obtained. As a typical example, we can mention the specific cases reported in the patterns a-4 and b-4. For the first one, the difference of chemical shift anisotropy and the total couplings are null, while for the second one, only the total couplings are averaged to zero. In addition the probability of detecting cases for which a particular numerical relation exists between T and $\Delta\Delta\sigma$ is lower than other situations for which nothing special occurs. In fact the type of spectral patterns which can be expected to be observed for a given carbon atom will strongly

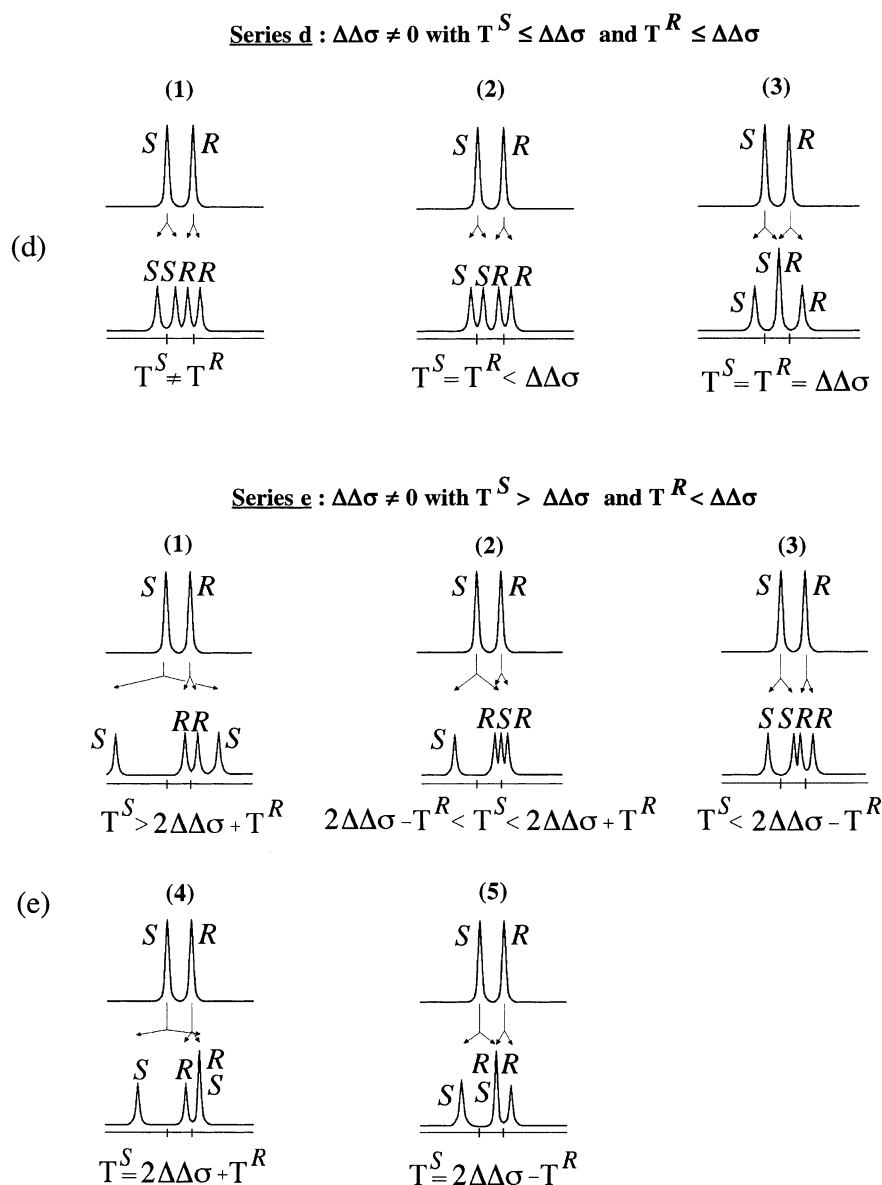


Figure 2. Schematic representation (series d and e) of possible enantiodifferentiation spectral patterns expected to be observed on the $^{13}\text{C}\text{-}\{^1\text{H}, \text{X}\}$ NMR spectra (top row) and $^{13}\text{C}\text{-}\{^1\text{H}\}$ NMR spectra (bottom row).

depend on its hybridization state and the internuclear distance $^{13}\text{C}\cdots^{31}\text{P}$. Thus, the cases shown in series a should be mainly detected for a pair of ^{31}P and ^{13}C nuclei directly bonded, when the carbon atom is hybridized sp^3 , while the cases presented in the series b and c should be seen when $\Delta\Delta\sigma$ is large, namely when the ^{13}C atom is hybridized sp or sp^2 . In contrast the cases described in the series d (T is small compared with $\Delta\Delta\sigma$) should be mainly detected for a pair of interacting ^{31}P and ^{13}C nuclei that are not directly bonded, but in which the ^{13}C atom is hybridized sp or sp^2 . Due to the versatility of anisotropic observables and the chiral discrimination mechanisms, no special predictions can be made when the magnitude of total couplings are larger or smaller than that of $\Delta\Delta\sigma$ (series e).

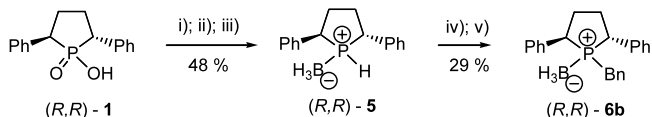
Finally, note that the various spectral patterns given in Figures 1 and 2 are general and valuable whatever the magnitude of the magnetic field used. However due to

the field-dependence of the CSA difference, the probability of observing spectral patterns with no CSA difference will be lower using very high magnetic fields.

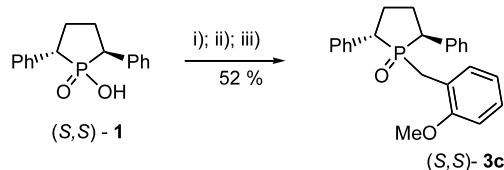
2.2. Synthesis of new chiral monophosphine oxide and borane derivatives

Requiring the use of precursors that could be handled and purified easily, the access to the air-sensitive phosphinolanes **4** led us to prepare intermediate phosphine borane **6** and phosphine oxide **3**. First precursors of our nucleophilic phosphines, compounds **6b** and **6c** were obtained after deprotonation by *n*-butyllithium (Scheme 2).

Due to the modest yield, we turned our investigations toward the preparation of phosphines oxides (Scheme 3). Thus, phenyl or methyl organo-copper reagents reacted with phosphinic chloride to give **3a** and **3d**.⁹



Scheme 2. Reagents and conditions: (i) $(\text{COCl})_2$, THF; (ii) LiAlH_4 ; (iii) $\text{BH}_3 \cdot \text{Me}_2\text{S}$, THF; (iv) 1 equiv. *n*-BuLi; (v) BnBr, THF.



Scheme 3. Reagents and conditions: (i) $(\text{COCl})_2$, THF; (ii) 2 equiv. $\text{LiAlH}_4(\text{O}-t\text{-Bu})_3$; (iii) $(2\text{-MeO})\text{C}_6\text{H}_4\text{CH}_2\text{-Br}$, THF.

The use of $\text{LiAlH}(\text{t-BuO})_3$ was necessary to obtain *P*-benzylated phosphine oxides **3b** and **3c** in satisfactory yields. After measurement of their enantiomeric purity by NMR in a CLC (these results are given in the following section), these precursors were cleanly and quantitatively converted into the corresponding phosphines by deprotection of boron group²⁰ or reduction.²¹

2.3. NMR results

The spectroscopic resolution of the phosphine borane **6b** was of interest for two reasons. For such kinds of compounds (especially the ones derived from poorly nucleophilic phosphines) HPLC may turn out to be unsuitable because a deprotection of the boron group may occur during the time of elution. The aim to propose an alternative method based on NMR analysis for e.e. measurement of phosphine boranes was therefore very pertinent. However, conversion of phosphine boranes to diastereomers through derivatization with some chiral auxiliary is difficult to achieve. Moreover, NMR analysis of enantiomers of **6b** with chiral lanthanide shift reagent [such as $\text{Eu}(\text{hfc})_3$]^{10b,22} or chiral solvating agents (such as *(R)*-(-)-(3,5-dinitrobenzoyl)- α -phenylethylamine)²³ met with no success in our hands. It must be noted that another advantage of the NMR involving COA's such as polypeptidic fibers is the very low reactivity of the chiral selector toward the solutes. In addition, whatever the amount of solute used in the preparation of the NMR sample, enantiomers can be always extracted from the NMR sample when the spectroscopic analysis is completed.

Figure 3a shows the $^{13}\text{C}\{-^1\text{H}\}$ signals (quoted VI, VII, and VIII) associated with three aromatic carbon atoms of benzyl group of $(\pm)\text{-6b}$ in the PBLG system at 310 K. The assignment of the aromatic signals is rather complex and was not performed. Note here that the analysis of results in terms of chiral discrimination does not require necessarily the exact assignment of resonances. The aromatic region shown in Figure 3a exhibits two distinct types of spectral patterns containing three and four lines. The nature of these patterns indicates that

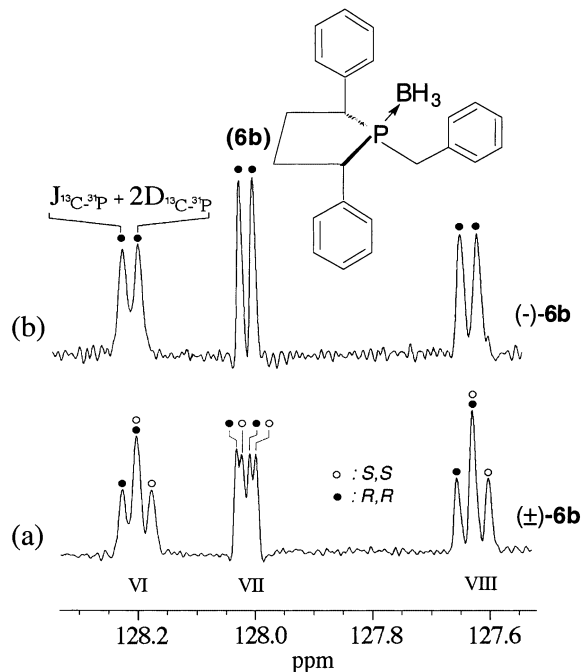


Figure 3. $^{13}\text{C}\{-^1\text{H}\}$ NMR signals associated with aromatic carbon atoms noted VI, VII and VIII of $(\pm)\text{-6b}$ (a) and $(-)\text{-6b}$ (b) and showing a chiral discrimination in the oriented system PBLG. The spectra a and b were recorded by adding 2500 and 3500 scans, respectively. A Gaussian filtering was applied to enhance the spectral appearance $\text{LB} = -1.8$ Hz, $\text{GB} = 60\%$ (a) and $\text{LB} = -3.0$ Hz, $\text{GB} = 58\%$ (b). Both spectra were zero-filled to 64 K points to increase the digital resolution. The peaks due to each enantiomer are labeled by (\bullet) and (\circ) .

corresponding carbon atoms are enantiodiscriminated, as well as illustrates the difficulty to predict a priori the spectral features of $^{13}\text{C}\{-^1\text{H}\}$ NMR signal for a given carbon in this type of compounds.

The two 'three-line' patterns can be seen as a triplet with 1:2:1 relative intensity, and hence can be compared in a first step with the second pattern given in the series a or the third one shown in the series d. Considering that the hybridized state of these ^{13}C atoms and the internuclear distance carbon-phosphorus is larger than 270 pm, we may a priori assume that the spectral figures for signals VI and VIII are rather related to the theoretical pattern d-3. To confirm our interpretation, we have recorded the $^{13}\text{C}\{-^1\text{H}\}$ NMR signals of $(-)\text{-6b}$ (e.e. >95%) using the same experimental conditions as for $(\pm)\text{-6b}$. As expected, the spectral patterns are much simpler since the signal of a single enantiomer is now detected. The comparison between both spectra allows calculation unambiguously of the terms $\Delta\Delta\sigma$, T^R and T^S . These values are given in Table 1, and perfectly agree with our speculations. The 'four-line' pattern of signal VII corresponds to the superposition of two independent doublets, one for each enantiomer. Here again the comparison between the spectrum of $(\pm)\text{-6b}$ and $(-)\text{-6b}$ enables comparison of this experimental spectral pattern with the theoretical pattern c-3. The spectral data for signal VII are given in Table 1.

Table 1. Spectral data associated with the aromatic carbon-13 atoms of (\pm)-**6b** recorded in the PBLG/CHCl₃ phase at 310 K

Signal ^a	I	II	III	IV	V	VI ^c	VII ^c	VIII ^c	IX	X	XI	XII
δ /ppm ^b	137.2	135.5	131.8	130.1	128.8	128.5	128.3	127.9	127.6	127.2	126.9	126.6
Assignment	Cq	Cq	Cq	CH	CH	CH	CH	CH	CH	CH	CH	CH
$ J_{^{13}\text{C}-^{31}\text{P}} $ /Hz	<2	4.3	4.7	4.2	2.0	1.1	4.0	1.8	3.5	2.3	2.7	2.4
$T_{^{13}\text{C}-^{31}\text{P}}^{S,S}$ /Hz	2.5	8.5	4.0	4.5	1.6	2.5	2.8	2.6	^d	1.6	2.3	2.3
$T_{^{13}\text{C}-^{31}\text{P}}^{R,R}$ /Hz	2.8	8.5	3.8	4.6	3.0	2.5	2.3	2.6	1.3	1.6	2.4	2.1
$ \Delta T_{^{13}\text{C}-^{31}\text{P}} $ /Hz	0.3	0	0.2	0.1	1.4	0	0.5	0	^d	0	0.1	0.2
$ \Delta\Delta\sigma_{^{13}\text{C}} $ /Hz	2.6	0	2.2	1.1	0.7	2.5	1.1	2.6	^d	0	2.3	2.2
Pattern	d-3	a-3	c-3	c-3	c-3	d-3	c-3	d-3	^d	a-3	d-3	d-3

^a The signals (I to XII) of aromatic carbon atoms are numbered from the most to the less deshielded.

^b Chemical shifts measured in chloroform.

^c The signal is shown in Fig. 3.

^d Ambiguous analysis by a lack of spectral resolution.

Although the spectral separations are not very large, the deconvolution of signals enables us to measure the enantiomeric excess with a good accuracy.

Encouraged by these first results, we have investigated two examples of chiral phosphine oxides such as derivatives **3b** and **3c**. Here again, neither the classical analytical NMR approaches (LCSR, CSA) nor chiral chromatographic methods (using our available chiral columns, e.g. Daicel, Chiracel[®] OD-H or Regis (*S,S*)-Whelk-O1) met with success. In a first assay, we have recorded the ¹³C-¹H spectrum of (\pm)-**3b** in an organic solution of PBLG. Surprisingly, the ability of the PBLG helices to orientate differentially the enantiomers of **3b** was not sufficient to provide separated resonances using ¹³C-¹H NMR. To date no clear explanations in terms of chiral discrimination mechanisms have been found to understand such a result. To improve the enantio-recognition toward a chiral solute, various solutions can be proposed. Thus, we can change either the temperature of the sample, the relative concentration of the components of the mixture, the organic solvent or the nature of polypeptide. In this work, this latter option has been explored, and has provided successful results.

Figures 4a and b show the ¹³C-¹H NMR signals associated with carbons C-2 and C-5 of (\pm)-**3b** and (-)-**3b** dissolved in a PCBL/CHCl₃ solution at 305 K. For these carbon atoms, two independent doublets centered on two different chemical shifts are observed. Contrary to the previous analysis, the C-2 and C-5 carbon atoms are now *sp*³ hybridized and directed bonded to the phosphorus atom. Consequently, the magnitude of ¹³C-³¹P total couplings is likely to be larger than the chemical shift anisotropy difference in this case, and hence the experimental patterns observed could be related to those of the series c. As expected, the comparison between the spectrum of (\pm)-**3b** and (-)-**3b** allows comparison of the experimental patterns of C-2 and C-5 with the theoretical patterns c-1 and c-3, respectively. The spectral data for all aliphatic ¹³C atoms of (\pm)-**3b** are reported in Table 2. As a second illustrative example involving a chiral monophosphine oxide, we have investigated the case of 1-(2-methoxyphenyl-

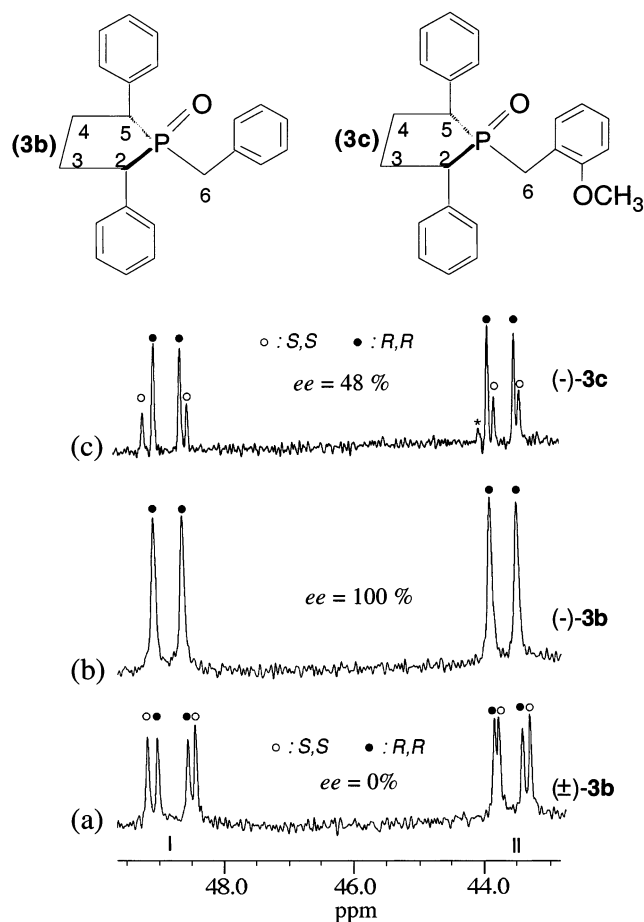


Figure 4. ¹³C-¹H NMR signals associated with C-2 and C-5 carbons of (\pm)-**3b** (a) and (-)-**3b** (b) as well as an enriched mixture of **3c** (*RR*-enriched, e.e.=48%) (c) in the oriented system PCBL. The spectra a, b and c were recorded by adding 15000, 15000 and 31000 scans, respectively. All spectra were zero-filled to 64 K points to increase the digital resolution. A Gaussian filtering was applied to enhance the spectral appearance LB=-5.0 Hz, GB=50% (a), LB=-4.0 Hz, GB=50% (b) and LB=-5 Hz, GB=40% (c). The peaks due to each enantiomer are labeled by (●) and (○).

methyl)-1-*r*-oxo-2-*c*,5-*t*-diphenylphospholane. The analysis of this compound is interesting because, disregarding the methoxy group, the molecular topology of **3c** is identical to that of **3b**. As a consequence, we may expect that the orientational behavior for both compounds in the chiral oriented phase will be very similar, thus leading to the same spectral patterns for each carbon atom. To check this assumption we have prepared a mixture of **3c** enriched in (*R,R*)-enantiomer (e.e.=48%). Figure 4c presents the $^{13}\text{C}\{-^1\text{H}\}$ signals I and II associated with carbon atoms C-2 and C-5 of **3c** enriched in (*R,R*)-enantiomer when the mixture is dissolved in a PCBL/CHCl₃ solution at 300 K. The large difference in peak intensity reveals immediately the enantiomeric enrichment of the mixture. Not surprisingly the spectral enantiodiscrimination patterns for C-2 and C-5 atoms are the same as for those observed for **3b**. A more extended analysis of dipolar data, summarized in Table 3, shows that the dipolar couplings for all *sp*³ carbon atoms are very similar in both compounds. This result demonstrates clearly that small changes in the molecular topology generate only very small changes in the orientational behavior between analogous derivatives. This occurrence is a very interesting point in view to performing systematic assignment of the absolute configuration in analogous series. Note in this example, that the slight difference of degree of polymerization for the polymer and the sample composition between **3b** and **3c** (concentrations in w/w) have no significant effects on the global orientational behavior of both compounds (see Table 5).

To explore the enantioselectivity of the PCBL as a chiral selector, we have recorded the $^{13}\text{C}\{-^1\text{H}\}$ NMR spectrum of chiral monophosphine oxides that do not possess a benzyl group bonded on the tetrahedral phosphorus atom. This case is typically afforded by compound **3d**, in which the benzyl group is replaced by a methyl group. It is clear that the global molecular topology as well as the electronic profile are now quite different from that associated with **3b** or **3c** as well as **6b**, and hence could modify the chiral discrimination mechanisms involved for this type of compounds. In Figure 5a, we report the $^{13}\text{C}\{-^1\text{H}\}$ NMR signals (noted I, II, III and IV) associated with the aliphatic carbon atoms (C-2 to C-5) of (\pm)-**3d**, dissolved in a PCBL/CHCl₃ solution at 300 K. Using the same analytical arguments than those presented for the analysis of **3b**, we may consider that the signals of C-2, C-5 atoms in the phospholane fragment belong to one of cases given in series c. As previously the comparison with the spectrum of the enantiopure derivative (*-*)-**3d** allows for relating unambiguously the experimental signals of C-2 (C-5) and C-5 (C-2) to the patterns c-3 and c-2, respectively (see Table 4). Note that for the C-5 atom, the experimental and theoretical patterns are inverted. This means that the algebraic relationship between T^S and T^R is simply inverted in this case, namely $T^R = 2\Delta\Delta\sigma + T^S$. The signal located about 32 ppm (carbon atom C-3 or C-4) is very particular because only two resonances with a large difference of peak intensity are observed. This case can be confidently related to the pattern b-2. It corresponds to a very specific spectral figure for which the $^{13}\text{C}\{-^31\text{P}\}$ total coupling for one enantiomer

Table 2. Spectral data associated with the aliphatic carbon-13 atoms of (\pm)-**3b** recorded in the PCBL/CHCl₃ phase at 305 K

Signal	I ^b	II ^b	III	IV	V
δ /ppm ^a	49.8	44.6	36.4	32.4	26.8
Assignment	C-2/C-5	C-5/C-2	C-6	C-3/C-4	C-4/C-3
$ J_{^{13}\text{C}-^{31}\text{P}} $ /Hz	57.6	60.4	56.4	7.5	9.3
$T_{^{13}\text{C}-^{31}\text{P}}^{S,S}$ /Hz	74.8	49.9	28.3	0	22.5
$T_{^{13}\text{C}-^{31}\text{P}}^{R,R}$ /Hz	46.8	44.5	53.7	4.8	15.3
$ \Delta T_{^{13}\text{C}-^{31}\text{P}} $ /Hz	28.0	19.0	25.4	4.8	7.2
$ \Delta\Delta\sigma_{^{13}\text{C}} $ /Hz	1.9	9.5	0.8	9.8	3.8
Pattern	c-1	c-3	c-1	b-3	c-2

^a Chemical shifts measured in chloroform.

^b The signal is shown in Fig. 4.

Table 3. Spectral data associated with the aliphatic ^{13}C atoms of (\pm)-**3c** recorded in the PCBL/CHCl₃ phase at 300 K

Signal	I ^b	II ^b	III	IV	V
δ /ppm ^a	50.0	44.3	32.4	29.0	26.6
Assignment	C-2/C-5	C-5/C-2	C-3/C-4	C-6	C-4/C-3
$ J_{^{13}\text{C}-^{31}\text{P}} $ /Hz	57.1	59.8	7.3	57.4	9.7
$T_{^{13}\text{C}-^{31}\text{P}}^{S,S}$ /Hz	72.2	42.7	0.0	35.7	15.5
$T_{^{13}\text{C}-^{31}\text{P}}^{R,R}$ /Hz	42.9	44.8	8.0	53.8	15.5
$ \Delta T_{^{13}\text{C}-^{31}\text{P}} $ /Hz	29.3	2.1	8.0	18.1	0
$ \Delta\Delta\sigma_{^{13}\text{C}} $ /Hz	3.5	9.7	0	9.0	0
Pattern	c-1	c-3	a-3	c-2	a-3

^a Chemical shifts measured in chloroform.

^b The signal is shown in Fig. 4 (top).

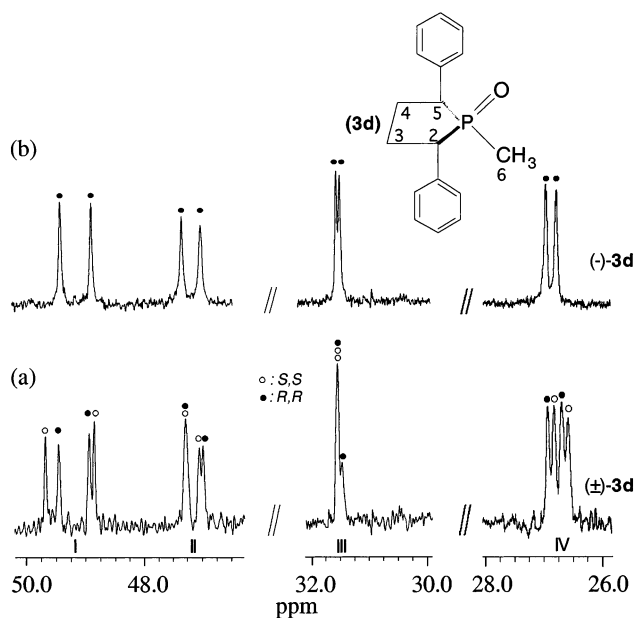


Figure 5. $^{13}\text{C}\{-^1\text{H}\}$ NMR signals associated with C-2 to C-5 carbon atoms of $(\pm)\text{-3d}$ (a) and $(-)\text{-3d}$ (b) showing a chiral discrimination in the oriented system PCBL. The spectra a and b were recorded by adding 30000, and 20000 scans, respectively. Spectra were zero-filled to 64 K points to increase the digital resolution. A Gaussian (LB = -3.0 Hz, GB = 20%) and Lorentzian (LB = 0.5 Hz) filtering were applied to enhance the spectral appearance of spectra (a) and (b). The peaks due to each enantiomer are labeled by (●) and (○).

(experimentally the (S,S) -isomer) is equal to zero ($J = -2\text{D}$) while the term T^R is equal to the difference of chemical shift between enantiomers, $\Delta\Delta\sigma$. Such a situation is a priori relatively rare but illustrates the complexity of spectral patterns when the magnitude of long-distance dipolar couplings (with a positive or negative sign) are close to the J couplings, leading to the same relative magnitude for T and $\Delta\Delta\sigma$. The most shielded signal shown in Fig. 5 (carbon atom C-4 or C-3) can be easily related to the spectral pattern c-4.

Finally we should note that the chemical shift difference, $\Delta\Delta\sigma$, for C-6 is 22.7 Hz (see Table 4). Regarding the hybridization state of this carbon (sp^3), this value is surprisingly large, and hence could suggest a strong

enantiodiscrimination for this carbon atom. For a better understanding of the origin of this effect, we may recast Eq. (2) in the principal frame (a', b', c') associated with a given carbon atom of the molecule, where the chemical shift tensor is diagonal. Thus, we obtain:^{13,19}

$$\Delta\sigma_{^{13}\text{C}}^{S \text{ or } R} = \frac{2}{3} \left[\sigma_{a'a'}^{S \text{ or } R} - \frac{1}{2} (\sigma_{b'b'}^{S \text{ or } R} + \sigma_{c'c'}^{S \text{ or } R}) \right] S_{a'a'}^{S \text{ or } R} + \frac{1}{3} (\sigma_{b'b'}^{S \text{ or } R} - \sigma_{c'c'}^{S \text{ or } R}) (S_{b'b'}^{S \text{ or } R} - S_{c'c'}^{S \text{ or } R}) \quad (5)$$

with

$$S_{\alpha'\alpha'}^{S \text{ or } R} = \sum_{\alpha, \beta = a, b, c} \cos \theta_{\alpha'\alpha}^{S \text{ or } R} \cos \theta_{\alpha'\beta}^{S \text{ or } R} S_{\alpha\beta}^{S \text{ or } R}$$

where $\theta_{\alpha'\alpha}$ are the angles between the principal axis system of the chemical shift tensor of a given carbon atom and the molecular frame. An examination of the relationship 5, shows that $\Delta\Delta\sigma$ is large when the order parameter differences ($S_{a'a'}^S - S_{a'a'}^R$) and $[(S_{b'b'}^S - S_{c'c'}^S) - (S_{b'b'}^R - S_{c'c'}^R)]$ are large.

3. Conclusion

Herein we report the modular synthesis of dialkyl- and trialkylphospholanes using phosphine boranes or phosphine oxides. For these both air-stable-precursors, $^{13}\text{C}\{-^1\text{H}\}$ NMR spectroscopy in CLC's reveals to be the method of choice to ascertain the configurational preservation of chiral heterocycle during the critical step consisting of the creation of the exocyclic phosphorus-carbon bond. Once in hand, they could be converted into the expected phospholanes via known reactions centered on the phosphorus atom. From a spectroscopic point of view, we have successfully explored the analytical potential of $^{13}\text{C}\{-^1\text{H}\}$ NMR spectroscopy using COAs in view to discriminating between enantiomers of chiral P -substituted 2,5-diphenyldiphenylphospholanes. In particular we have shown the ability of PCBL helices to orientate differentially such enantiomers, and hence this work is the first practical example of an application of this chiral polypeptide as a COA. These results also emphasize that organic solutions of PCBL are very efficient enantioselective oriented media, and hence they provide an interesting alternative to organic solutions of PBLG,

Table 4. Spectral data associated with the aliphatic ^{13}C atoms of $(\pm)\text{-3d}$ recorded in the PCBL/CHCl₃ phase at 300 K

Signal	I ^b	II ^b	III ^b	IV ^b	V
δ/ppm^a	49.5	47.4	31.9	27.3	13.9
Assignment	C-2/C-5	C-5/C-2	C-3/C-4	C-4/C-3	C-6
$ J_{^{13}\text{C}-^{31}\text{P}} /\text{Hz}$	60.8	61.5	7.2	8.8	63.4
$ T_{^{13}\text{C}-^{31}\text{P}}^{S,S} /\text{Hz}$	85.1	26.5	0	21.5	23.1
$ T_{^{13}\text{C}-^{31}\text{P}}^{R,R} /\text{Hz}$	53.3	32.6	6.5		
	21.5	68.4			
$ \Delta T_{^{13}\text{C}-^{31}\text{P}} /\text{Hz}$	31.8	6.1	6.5	0	45.3
$ \Delta\Delta\sigma_{^{13}\text{C}} /\text{Hz}$	7.4	3.1	3.2	9.8	22.7
Pattern	c-3	c-2	b-2	c-4	c-2

^a Chemical shifts measured in chloroform.

^b The signal is shown in Fig. 5.

when these latter gave rather poor results. Besides, we have proved that this method is very adapted to analyze sensitive chiral compounds susceptible to be rapidly degraded by other approaches such as GC or HPLC. Here again, we have illustrated the advantages of this method in terms of rapidity, sensibility and versatility compared with conventional methods used so far.

4. Experimental

4.1. Synthetic procedures

The 2-(bromoethyl)anisole was prepared from the corresponding alcohol according to Corey's procedure.²⁴ Racemic and enantiomerically pure 1-hydroxy-1-*r*-oxo-2-*c*,5-*t*-diphenylphospholane **1**, 1-*r*-oxo-2-*c*,5-*t*-diphenylphospholane **2** were prepared according to the reported procedure.⁸

4.1.1. General. All reactions and manipulations were performed under a dry argon atmosphere using standard Schlenk-type techniques. Solvents were purified appropriately before use. Melting points are uncorrected. Routine ¹H, ³¹P-¹H and ¹³C-¹H NMR spectra in isotropic solvents were recorded on a Bruker AC 250 apparatus equipped with a QUAD probehead. Chemical shifts are reported in δ (ppm) referenced to the residual CHCl₃ (¹H signal at 7.26 ppm, and CDCl₃ ¹³C signal at 77.0 ppm). HPLC analyses were performed on a Spectra-Physics P100-UV100 HPLC system with detection at $\lambda=254$ nm and equipped with a chiral column Chiralcel OD-H from Daicel Chemical Industries Ltd. Mixtures of hexane and isopropanol were used for elution. GC-MS analyses were carried out on a OK1 DP 125 gas chromatograph equipped with a CPSil quartz capillary column and connected to a Riber Mag R10-10 mass detector. High resolution mass spectra (HRMS) and electrospray mass spectra were obtained on a Finnigan-MAT-95-S spectrometer.

4.1.2. (S,S)-(-)-1-*r*-Oxo-1,2-*c*,5-*t*-triphenylphospholane **3a, (S,S)-(-)-1-benzyl-1-*r*-oxo-2-*c*,5-*t*-diphenylphospholane **3b** and (S,S)-(-)-1-methyl-1-*r*-oxo-2-*c*,5-*t*-diphenylphospholane **3d**.** Compounds **3a**, **3b** and **3d** were prepared using procedures described in Ref. 8.

4.1.3. (S,S)-(-)-1-(2-Methoxyphenylmethyl)-1-*r*-oxo-2-*c*,5-*t*-diphenylphospholane **3c.** (S,S)-1-Chloro-1-*r*-oxo-2-*c*,5-*t*-diphenylphospholane (3.68 mmol, from 1 g of (S,S)-(-)-1-hydroxy-1-*r*-oxo-2-*c*,5-*t*-diphenylphospholane, $[\alpha]_D^{20} = -103$ (*c* 0.6 CH₂Cl₂), was suspended in 30 mL of freshly distilled ether after sonication and cooled at 0°C. Lithium tri-*tert*-butoxyaluminumhydride (12 mmol, prepared from 455 mg (12 mmol) of lithium aluminum hydride and 2.66 g (36 mmol) of *t*-butanol) in suspension in ether were then added via cannula and the mixture was allowed to reach rt. When the gas evolution has ceased, 2-(bromomethyl)anisole (1.30 g, 6.5 mmol) was added and the resulting mixture was stirred overnight. After dilution with EtOAc (30 mL) the solution was hydrolyzed with HCl (1 M). The

aqueous phase was extracted several times with EtOAc and the combined organic layers were washed with aqueous saturated K₂CO₃, then distilled water and dried over MgSO₄. The crude product was purified by flash chromatography on silica gel (EtOAc/CH₂Cl₂: 75/25; *R*_f 0.72) and recrystallized in a dichloromethane/EtOAc mixture. After slow evaporation of the solvent, 723 mg (52%) of colorless needles were obtained (mp = 135–137°C. $[\alpha]_D^{20} = -49.8$ (*c* 0.85 CH₂Cl₂). ¹H NMR (250 MHz, CDCl₃): δ 7.50–7.30 (4H, m), 7.35–7.25 (1H, d, *J* = 7.9), 7.20–7.05 (4H, m), 7.00–6.95 (1H, d, *J* = 7.9), 6.90–6.80 (3H, m), 6.80–6.70 (1H, t, *J* = 7.9), 3.80 (3H, s), 3.80–3.60 (1H, m), 3.10–3.00 (2H, m), 2.70–2.55 (1H, m), 2.55–2.20 (3H, m). ¹³C NMR (62.9 MHz, CDCl₃): δ 156.7 (s), 136.9 (d, *J* = 5.3), 136.4 (s), 132.2 (d, *J* = 4.3), 129.2 (s), 129.1 (d, *J* = 5), 128.7 (s), 128.5 (s), 127.7 (d, *J* = 4.2), 127.3 (s), 126.7 (s), 121.4 (s), 120.1 (d, *J* = 7.6), 110.7 (s), 55.8 (s), 50.0 (d, *J* = 57.1), 44.3 (d, *J* = 59.8), 32.4 (d, *J* = 7.3), 29.0 (d, *J* = 57.4), 26.6 (d, *J* = 9.7). ³¹P NMR (101.2 MHz, CDCl₃): δ 59.6 (s). HRMS (EI) *m/z* calcd for [C₂₄H₂₅O₂P]⁺: 376.1592, found 376.1583. Anal. calcd for C₂₄H₂₅O₂P: C, 76.58; H, 6.69, found: C, 75.76; H, 6.66.

4.1.4. (R,R)-2-*c*,5-*t*-Diphenylphospholane borane **5.** To a suspension of 3.7 mmol of (R,R)-1-chloro-1-*r*-oxo-2-*c*,5-*t*-diphenylphospholane (prepared by reaction of oxalyl chloride to 1 g (3.7 mmol) of the corresponding phosphinic acid) in 50 mL diethyl ether were added portionwise LiAlH₄ (190 mg, 5 mmol) under vigorous stirring. The solution turned yellow, then violet. In the case where the solution remains yellow after the addition of the amount, an additional amount of LiAlH₄ was added until the solution turns violet. The mixture was stirred overnight, and degassed water was dropped into the gently stirred mixture until the aluminum salts collapse. The supernatant solution was transferred via cannula into a Schlenk tube. The precipitated salts were washed with 10 mL of dry, degassed diethyl ether. Borane-dimethylsulfide complex was then added and the resulting solution stirred for 2 h at rt. Work up (1 M HCl hydrolysis, diethyl ether extraction, washing of the ethereal extract with salted water, drying over MgSO₄ and evaporation) afforded the expected compound (0.45 g of a white solid) which was used without further purification when no corresponding secondary phosphine oxide was detected by ³¹P NMR (otherwise, purification by flash chromatography (pentane/ether: 95/5), yield 50%). ¹H NMR (250 MHz, CDCl₃): δ 7.40–7.21 (10H, m), 4.79 (1H, dd, *J*_{P-H} = 358 Hz, *J* = 7.5 Hz), 4.05–3.85 (1H, m), 3.6–3.45 (1H, m), 2.70–2.51 (2H, m), 2.30–2.15 (2H, m), 0.41 (3H, q (large), *J* = 100 Hz). ³¹P NMR (101.2 MHz, CDCl₃): δ 29.4 (broad d, *J* ≈ 42 Hz). MS (EI, 70 eV): 78 (37.23) 91 (81) 104 (30) 117 (53) 123 (33) 136 (40) 240 (100. M-BH₃).

4.1.5. (R,R)-(-)-1,2-*c*,5-*t*-Triphenylphospholane borane **6a.** A suspension of anhydrous cerium chloride (1.23 g, 5 mmol) in 20 mL THF was stirred for 2.5 h. A solution of (-)-1-*r*-oxo-1,2-*c*,5-*t*-triphenylphospholane (830 mg, 2.5 mmol) in 30 mL THF was then added. After 1 h stirring, the milky suspension was cooled to

0°C, and LiAlH₄ (114 mg, 3 mmol) was added portionwise under a stream of argon. The gray suspension was stirred for 16 h at rt and 2 M borane–dimethylsulfide (1.5 mL, 3 mmol) in THF was added dropwise. After 2 h stirring, the reaction mixture was hydrolyzed with water until a precipitate was obtained. The mixture was filtered, the filtrate was then washed with saturated NH₄Cl solution (2×50 mL), the aqueous phases extracted with dichloromethane, and the combined organic phases dried over magnesium sulfate. Removal of the solvents left a white solid (850 mg) which was purified by silica chromatography (pentane/ether 95/5 then 80/20) to give a white solid (709 mg, 86%); mp=99–101°C (the racemic material prepared according to the same procedure showed mp=182°C, $[\alpha]_D^{20} = -116$ (*c* 1.65 CHCl₃). ¹H NMR (250 MHz, CDCl₃): δ 7.41–7.20 (4H, m), 7.21–7.00 (9H, m), 6.87 (2H, d, *J*=6.8), 4.04 (1H, dt, *J*=10.8; *J*=7.8), 3.80 (1H, ddd, *J*=17.8; 12.0; 5.7), 2.70–2.80 (1H, m), 2.20–2.30 (2H, m), 2.15–2.01 (1H, m). ¹³C NMR (62.9 MHz, CDCl₃): δ 131.6 (d, *J*=2.8), 131.2 (d, *J*=8.3), 128.8 (d, *J*=5.1), 128.6 (d, *J*=1.8), 128.2 (d, *J*=2.3), 128.0 (d, *J*=11.6), 127.1 (d, *J*=5.1), 127.0 (d, *J*=1.9), 126.3 (d, *J*=2.8), 51.0 (d, *J*=61.5), 46.7 (d, *J*=62), 31.5 (d, *J*=7.4), 27.9 (d, *J*=8.3). ³¹P NMR (101.2 MHz, CDCl₃): δ 21.3.

4.1.6. (R,R)-(-)-1-Benzyl-2-*c*,5-*t*-diphenylphospholane borane 6b. Commercial *n*-BuLi (1.6 M) in hexane (1.1 mL, 1.8 mmol) was added dropwise to a solution of (R,R)-2-*c*,5-*t*-diphenylphospholane borane **5** (450 mg, 1.8 mmol) in 30 mL dry THF, at -78°C. The solution turned yellow when an equivalent of *n*-BuLi was added. The solution was stirred at -78°C for 5 min, then benzyl bromide (210 mL, 1.8 mmol) was added at this temperature. The mixture was left to reach rt and stirred overnight. After dilution with diethyl ether (30 mL) the solution was hydrolyzed with HCl (1 M). The aqueous phase was extracted several times with diethyl ether. The combined organic extracts were washed (water), dried (MgSO₄) and concentrated to give 230 mg of an oil which was purified by flash chromatography on silica gel (pentane/ether: 90/10), affording 180 mg (29%) of a solid (mp=125–130°C. $[\alpha]_D^{20} = -57.2$ (*c* 1.03 MeOH). ¹H NMR (250 MHz, CDCl₃): δ 7.55–7.2 (11H, m), 7.11–7.02 (2H, m), 6.75–6.65 (2H, m), 3.80–3.70 (1H, m), 3.40–3.30 (1H, m), 2.65 (1 H, s), 2.60 (1H, s), 2.60–2.45 (2H, m), 2.30–2.15 (2H, m), 1.15–0.21 (3H, m). ¹³C NMR (62.9 MHz, CDCl₃): δ 137.2 (d, *J*<2), 135.5 (d, *J*=4.3), 131.8 (d, *J*=4.7), 130.1 (d, *J*=4.2), 128.8 (d, *J*=2.0), 128.5 (d, *J*=1.1), 128.3 (d, *J*=4.0), 127.9 (d, *J*=1.8), 127.6 (d, *J*=3.5), 127.2 (d, *J*=2.3), 126.9 (d, *J*=2.7), 126.6 (d, *J*=2.4), 46.2 (d, *J*=29.6), 47.8 (d, *J*=26.8), 33.1 (d, *J*=3.7), 30.7 (d, *J*=23.1), 29.8 (s). ³¹P NMR (101.2 MHz, CDCl₃): δ 41.5 (broad d, *J*≈58 Hz). HRMS (EI) *m/z* calcd for [C₂₃H₂₆BP]⁺: 344.1865, found: 344.1863.

4.1.7. (S,S)-(+)-1-*r*-(2-Methoxyphenylmethyl)-2-*c*,5-*t*-diphenylphospholane borane 6c. Same procedure as above using (S,S)-2-*c*,5-*t*-diphenylphospholane borane **5** (3.7 mmol) and 2-(chloromethyl)-anisole (575 mg, 3.67 mmol) as electrophile. The crude material was purified by flash chromatography on alumina (pentane/

ether: 80/20), then recrystallized (EtOAc/cyclohexane) to give 350 mg (25%) of colorless crystals (mp=132–135°C, $[\alpha]_D^{20} = +40.7$ (*c* 0.84 CH₂Cl₂). ¹H NMR (250 MHz, CDCl₃): δ 7.50–7.45 (2H, d, *J*=7.9), 7.45–7.35 (2H, t, *J*=7.9), 7.35–7.25 (1H, d, *J*=7.9), 7.25–7.15 (1H, d, *J*=7.9), 7.15–7.05 (3H, m), 6.95–6.75 (3H, m), 6.70–6.60 (2H, m), 3.80 (3H, s), 3.80–3.60 (1H, m), 3.45–3.25 (1H, m), 3.05 (1H, t, *J*=17), 2.55–2.05 (5H, m), 1.21–0.05 (3 H). ¹³C NMR (62.9 MHz, CDCl₃): δ 156.8 (s), 137.4 (s), 136.0 (s), 132.0 (s), 128.7 (d, *J*=2), 128.4 (d, *J*=4.8), 128.3 (d, *J*=2.3), 127.9–127.8 (3C, m), 127.0 (d, *J*=3.7), 127 (d, *J*=2.4), 126.4 (d, *J*=2.6), 120.7 (s), 110.3 (s), 55.2 (s), 46.5 (d, *J*=28.5), 43.3 (d, *J*=26.3), 33.2 (s), 29.9 (s), 23.4 (d, *J*=24.4). ³¹P NMR (101.2 MHz, CDCl₃): δ 42.4 (broad d, *J*≈54 Hz). HRMS (EI) *m/z* calcd for [C₂₄H₂₈BOP]⁺: 374.1960, found: 374.20.

4.1.8. (S,S)-(-)-1-*r*-Benzyl-2-*c*,5-*t*-diphenylphospholane 4b. This synthesis has been reported in Ref. 8.

4.1.9. (S,S)-1-*r*-(2-Methoxyphenylmethyl)-2-*c*,5-*t*-diphenylphospholane 4c. (a) By reduction from the corresponding oxide. In a Schlenk tube under argon, (S,S)-(-)-1-(2-methoxyphenylmethyl)-1-*r*-oxo-2-*c*,5-*t*-diphenylphospholane (711 mg, 1.9 mmol) was suspended in freshly distilled DME (3 mL) at rt. Methyl triflate (0.235 mL, 2.1 mmol) was then added. After 2 h at rt, the homogeneous solution was cooled to 0°C and lithium aluminum hydride (180 mg, 4.75 mmol) was added portionwise. The reaction mixture was allowed to warm to rt and stirred for additional 1.5 h. After dilution with dried and degassed ether, the mixture was filtered under argon through silica via cannula. The solvent was removed in vacuo and the phospholane was obtained as a white solid and stored in a glove box without any further purification.

(b) By deprotection of the boron group. All solvents and aqueous solutions were previously degassed. Reaction and work-up were performed under argon atmosphere. In a Schlenk tube (S,S)-1-*r*-(2-methoxyphenylmethyl)-2-*c*,5-*t*-diphenylphospholane borane (410 mg, 1.1 mmol) was solubilized in freshly distilled dichloromethane (10 mL) at rt. HBF₄·Et₂O (0.820 mL, 11 mmol) was then added and the mixture was stirred overnight. After dilution with dry ether (20 mL) and cooling to 0°C, NaHCO₃ satd (5 mL) was added. After ca. 10 min of vigorous stirring, the organic layer was separated and the aqueous layer was extracted with ether (5 mL). The combined organic layers were washed with distilled water and dried over MgSO₄. After evaporation, the expected phosphine was obtained as a white solid. ¹H NMR (250 MHz, CDCl₃): δ 7.55–7.25 (11H, m), 7.45–7.25 (4H, m), 7.25–7.10 (3H, m), 7.10–7.00 (2H, m), 7.00–6.90 (2H, d, *J*=6.7), 6.80–6.70 (3H, m), 3.80–3.70 (4H), 3.45–3.35 (1H, m), 2.75 (1H, dd, *J*=4.8, 13), 2.65–2.30 (3H, m), 2.20 (1H, dd, *J*=4.5, 13), 2.00–1.85 (1H, m). ¹³C NMR (62.9 MHz, CDCl₃): δ 140.0 (s), 132.3 (s), 130.8 (d, *J*=5.9), 128.8–128.4 (m), 128.4–128.0 (m), 127.9 (s), 127.2 (s), 126.1 (s), 125.8 (s), 120.8 (s), 110.7 (s), 55.6 (s), 49.1 (d, *J*=18.7), 47.5 (d,

Table 5. Compositions of liquid-crystalline NMR samples investigated

Sample	Solute	Stereochemistry	Polymer	DP ^a	Co-solvent	Solute/mg ^b	Polymer/mg ^b	Co-solvent/ mg ^b	% of polymer in weight
1	3b	(±)	PBLG	562	CHCl ₃	98	120	510	16.5
2	3b	(–)	PBLG	562	CHCl ₃	100	120	509	16.5
3	3c	(±)	PCBLL	992	CHCl ₃	30	102	405	19.0
4	3c	(–)	PCBLL	992	CHCl ₃	30	101	405	19.0
5	3d	(–) 48% e.e.	PCBLL	1100	CHCl ₃	5/14	120	599	16.3
6	6b	(±)	PCBLL	1100	CHCl ₃	9	101	600	14.2
7	6b	(–)	PCBLL	1100	CHCl ₃	9	101	602	14.1

^a DP: Degree of polymerization of polypeptide used.

^b The accuracy on the weighting is ±1 mg.

$J=17.4$), 36.7 (s), 32.4 (s), 26.2 (d, $J=26.7$). ³¹P NMR (101.2 MHz, CDCl₃): δ 18.8.

4.2. NMR spectroscopy in chiral oriented solvents

The CLC NMR samples were prepared using around 100 mg of homopolypeptide (commercially available from Sigma), 10–100 mg of chiral material, and around 550 mg of organic solvent directly weighted into a 5 mm o.d. NMR tube. The exact composition of each oriented NMR sample is given in Table 5. All NMR tubes were sealed to avoid solvent evaporation and centrifuged back and forth until an optically homogeneous birefringent phase was obtained. Various experimental details on the method can be found in Ref. 13. The ¹³C-¹H 1D NMR experiments were performed at 9.4 T on a Bruker DRX 400 high-resolution spectrometer equipped with a dual ¹³C/¹H probe operating at 100.6 MHz for ¹³C and with a standard variable temperature unit (BVT 3000). In order to remove the proton-¹³C scalar and dipolar couplings, the protons were broadband decoupled using WALTZ-16 composite pulse sequence. Other experimental NMR parameters or details are given in the figure captions.

References

- Komarov, I. V.; Börner, A. *Angew. Chem., Int. Ed. Engl.* **2001**, *40*, 1197.
- (a) Hayashi, T. *J. Organomet. Chem.* **1999**, *576*, 195; (b) Lagasse, F.; Kagan, H. B. *Chem. Pharm. Bull.* **2000**, *48*, 315.
- Dalko, P. I.; Moisan, L. *Angew. Chem., Int. Ed. Engl.* **2001**, *40*, 3726 and references cited therein.
- (a) Vedejs, E.; Daugulis, O. *J. Am. Chem. Soc.* **1999**, *121*, 5813; (b) Vedejs, E.; Daugulis, O.; McKay, J. A.; Rozners, E. *Synlett* **2001**, *10*, 1499.
- (a) Zhang, C.; Lu, X. *J. Org. Chem.* **1995**, *60*, 2906; (b) Zhu, G.; Chen, Z.; Jiang, Q.; Xiao, D.; Cao, P.; Zhang, X. *J. Am. Chem. Soc.* **1997**, *119*, 3836.
- Xu, Z.; Lu, X. *Tetrahedron Lett.* **1999**, *40*, 549.
- Alvarez-Ibarra, C.; Csaky, A. G.; Gomez de la Oliva, C. *J. Org. Chem.* **2000**, *65*, 3544.
- Guillen, F.; Rivard, M.; Toffano, M.; Legros, J.-Y.; Daran, J.-C.; Fiaud, J.-C. *Tetrahedron* **2002**, *58*, 5895.
- (a) Guillen, F.; Moinet, C.; Fiaud, J.-C. *Bull. Soc. Chim. Fr.* **1997**, *134*, 371; (b) Blake, A. J.; Hume, S. C.; Li, W. S.; Simpkins, N. S. *Tetrahedron* **2002**, *58*, 4589.
- (a) Parker, D. *Chem. Rev.* **1991**, *91*, 1441; (b) Rothchild, R. *Enantiomer* **2000**, *5*, 457; (c) Finn, M. G. *Chirality* **2002**, *14*, 534.
- Fuchs, G.; Doguet, L.; Barth, D.; Perrut, M. *J. Chromatogr.* **1992**, *623*, 329.
- (a) Dunach, E.; Kagan, H. B. *Tetrahedron. Lett.* **1985**, *26*, 2649; (b) Toda, F.; Toyotaka, R.; Fukuda, H. *Tetrahedron: Asymmetry* **1990**, *2*, 303.
- Sarfati, M.; Lesot, P.; Merlet, D.; Courtieu, J. *Chem. Commun.* **2000**, 2069 and references cited therein.
- Aroulanda, C.; Sarfati, M.; Courtieu, J.; Lesot, P. *Enantiomer* **2001**, *6*, 281.
- Lesot, P.; Sarfati, M.; Courtieu, J. *Chem. Eur. J.*, in press.
- Lesot, P.; Merlet, D.; Sarfati, M.; Courtieu, J.; Zimmermann, H.; Luz, Z. *J. Am. Chem. Soc.* **2002**, *124*, 10071.
- Lesot, P.; Merlet, D.; Meddour, A.; Loewenstein, A.; Courtieu, J. *Faraday Trans.* **1995**, *91*, 1371.
- Meddour, A.; Berdagué, P.; Hedli, A.; Courtieu, J.; Lesot, P. *J. Am. Chem. Soc.* **1997**, *119*, 4502.
- Emsley, J. W.; Lindon, J. C. *NMR Spectroscopy Using Liquid Crystal Solvents*; Pergamon Press: Oxford, 1975.
- McKinstry, L.; Livinghouse, T. *Tetrahedron* **1995**, *51*, 7655.
- Imamoto, T.; Kikuchi, S. I.; Miura, T.; Wada, Y. *Org. Lett.* **2001**, *3*, 87.
- Sullivan, G. R. *Top. Stereochem.* **1979**, *10*, 287.
- Dunach, E.; Kagan, H. B. *Tetrahedron Lett.* **1985**, *26*, 2649.
- Corey, E. J.; Kirst, H. A.; Katzenellenbogen, J. A. *J. Am. Chem. Soc.* **1970**, *92*, 6314.